

# Molecular Nanostructures on the Surface of a $d_{x^2-y^2}$ -Superconductor

Roy H. Nyberg and Dirk K. Morr

Department of Physics, University of Illinois at Chicago, Chicago, IL 60607

(Dated: November 20, 2018)

We study molecular nanostructures on the surface of a  $d_{x^2-y^2}$ -wave superconductor. We show that the interplay between the molecular nanostructure's internal excitation spectrum and quantum interference of the scattered host electrons leads to a series of novel effects in the local density of states. We demonstrate that these effects give insight into both the nature of the superconducting pairing correlations and of the intermolecular interactions.

PACS numbers: 73.22.-f, 73.22.Gk, 74.72.-h

Nanostructures provide the intriguing possibility of manipulating in a controlled way the electronic structure of the host system they reside on [1]. This level of control opens new venues for studying the complex electronic structure of many strongly correlated electron systems. For example, it was suggested that nanostructures can elucidate the nature of superconducting correlations in conventional [2] and unconventional superconductors [3]. Nanostructures formed from more complex building blocks, such as molecules with internal degrees of freedom, provide a novel way of manipulating and simultaneously gaining insight into the electronic structure of complex systems. The internal vibrational and rotational excitations of single molecules have been intensively studied by inelastic tunneling spectroscopy [4, 5]. Their interaction with and effect on the electronic structure of a metallic surface was recently investigated by Gross *et al.* [6].

In this Letter we study nanostructures composed of two molecules that reside on the surface of an unconventional  $d_{x^2-y^2}$ -superconductor that represents the family of high-temperature superconductors (HTSC). We show that the interplay between the molecular nanostructure's internal excitation spectrum and quantum interference of the scattered host electrons leads to a series of novel effects in the local density of states (LDOS) of the superconductor. Our main results are threefold. First, we identify three types of intermolecular interactions and show that each of them leads to *qualitatively* distinguishable features in the LDOS. This, in turn, allows one to identify the nature of intermolecular interaction from experimental measurements of the LDOS. Second, we demonstrate that the LDOS changes with the molecules' distance and orientation relative to the underlying host lattice. This effect permits us to probe the spatial dependence of superconducting correlations. Third, we show that by exciting specific energy levels of the molecular structure, the LDOS can be manipulated in a controlled manner. These results intricately relate the study of strongly correlated electron systems with the further development of molecular electronics.

A nanostructure consisting of  $N$  molecules, represented by local bosonic modes [7], on the surface of a two-

dimensional  $d_{x^2-y^2}$  superconductor possesses the Hamiltonian  $H = H_e + H_b + H_{int}$  where

$$\begin{aligned} H_e &= \sum_{\mathbf{k}, \sigma=\uparrow, \downarrow} \epsilon_{\mathbf{k}} c_{\mathbf{k}, \sigma}^\dagger c_{\mathbf{k}, \sigma} + \sum_{\mathbf{k}} \Delta_{\mathbf{k}} c_{\mathbf{k}, \uparrow}^\dagger c_{-\mathbf{k}, \downarrow}^\dagger + h.c. , \\ H_b &= \omega_0 \sum_i a_{\mathbf{r}_i}^\dagger a_{\mathbf{r}_i} + J \sum_{i,j} \Psi [a_{\mathbf{r}_i}^\dagger, a_{\mathbf{r}_i}, a_{\mathbf{r}_j}^\dagger, a_{\mathbf{r}_j}] , \\ H_{int} &= g \sum_{i, \sigma} (a_{\mathbf{r}_i}^\dagger + a_{\mathbf{r}_i}) c_{\mathbf{r}_i, \sigma}^\dagger c_{\mathbf{r}_i, \sigma} . \end{aligned} \quad (1)$$

$H_e$  and  $H_b$  describe the unperturbed superconductor and nanostructure, respectively, and  $H_{int}$  represents the interaction between them.  $c^\dagger, a^\dagger$  are the fermionic and bosonic creation operators, respectively.  $\Delta_{\mathbf{k}} = \Delta_0 (\cos k_x - \cos k_y) / 2$  is the  $d_{x^2-y^2}$ -wave superconducting gap and  $\epsilon_{\mathbf{k}} = -2t (\cos k_x + \cos k_y) - 4t' \cos k_x \cos k_y - \mu$  is the normal state tight-binding dispersion.  $\omega_0$  is the characteristic frequency of the  $N$  modes located at  $\mathbf{r}_i$  ( $i = 1, \dots, N$ ).  $\Psi$  is a quadratic functional in the bosonic operators and describes the interaction between modes at sites  $\mathbf{r}_i$  and  $\mathbf{r}_j$  with strength  $J$  (three specific forms of  $\Psi$  are discussed below).  $g$  is the boson-fermion scattering vertex. The fermionic Green's function of the unperturbed (clean) system in Nambu notation is

$$\hat{G}_0^{-1}(\mathbf{k}, i\omega_n) = [i\omega_n \tau_0 - \epsilon_{\mathbf{k}} \tau_3] \sigma_0 + \Delta_{\mathbf{k}} \tau_2 \sigma_2 , \quad (2)$$

where  $\sigma_i$  and  $\tau_i$  are the Pauli matrices in spin and Nambu space, respectively. Diagonalizing  $H_b$  via a Bogoliubov transformation to new operators  $b_l^\dagger, b_l$  ( $l = 1, \dots, N$ ), one obtains  $H_b = \sum_l \Omega_l b_l^\dagger b_l$  and

$$H_{int} = \sum_{i, l, \sigma} g_{\mathbf{r}_i}^{(l)} (b_l^\dagger + b_l) c_{\mathbf{r}_i, \sigma}^\dagger c_{\mathbf{r}_i, \sigma} , \quad (3)$$

where  $g_{\mathbf{r}_i}^{(l)}$  is a site and mode dependent interaction vertex, and  $\Omega_l$  is the bosonic energy spectrum. The full fermionic Green's function is now given by

$$\begin{aligned} \hat{G}(\mathbf{r}, \mathbf{r}', \omega_n) &= \hat{G}_0(\mathbf{r}, \mathbf{r}', \omega_n) + \sum_{i,j} \hat{G}_0(\mathbf{r}, \mathbf{r}_i, \omega_n) \\ &\quad \times \hat{\Sigma}(\mathbf{r}_i, \mathbf{r}_j, \omega_n) \hat{G}_0(\mathbf{r}_j, \mathbf{r}', \omega_n) , \end{aligned} \quad (4)$$

where  $\hat{\Sigma}$  is the full fermionic self-energy obtained from the Bethe-Salpeter equation

$$\hat{\Sigma}(\mathbf{r}_i, \mathbf{r}_j, \omega_n) = \hat{\Sigma}_0(\mathbf{r}_i, \mathbf{r}_j, \omega_n) + \sum_{p,q} \hat{\Sigma}_0(\mathbf{r}_i, \mathbf{r}_p, \omega_n) \times \hat{G}_0(\mathbf{r}_p, \mathbf{r}_q, \omega_n) \hat{\Sigma}(\mathbf{r}_q, \mathbf{r}_j, \omega_n) \quad (5)$$

with  $p, q = 1, \dots, N$  and

$$\hat{\Sigma}_0(\mathbf{r}_i, \mathbf{r}_j, \omega_n) = T \sum_{m,l} \tau_3 g_{\mathbf{r}_i}^{(l)} \hat{G}_0(\mathbf{r}_i, \mathbf{r}_j, \omega_n + \nu_m) \times D_l(\nu_m) \tau_3 g_{\mathbf{r}_j}^{(l)}. \quad (6)$$

The retarded form of the bosonic propagator is given by

$$D_l^R(\omega) = [\omega + i\Gamma(\omega) - \Omega_l]^{-1} - [\omega + i\Gamma(\omega) + \Omega_l]^{-1}. \quad (7)$$

The lowest order vertex corrections scale as  $\delta g/g \sim (gk_F/4v_F)^2 F$  where  $F$  is a function of  $O(1)$  for bosonic and fermionic frequencies smaller than  $\Delta_0$  [8]. For the parameter range considered below,  $gk_F/4v_F \ll 1$  and vertex corrections can thus be neglected. The interaction,  $H_{int}$ , not only leads to changes in the fermionic LDOS, but also affects the bosonic excitation spectrum twofold. First,  $H_{int}$  shifts the unperturbed bosonic frequencies, a shift that we take to be included in the effective values for  $\Omega_l$  considered below. Second, the bosonic modes acquire a finite lifetime,  $\Gamma(\omega) \neq 0$ . The lowest order bosonic self-energy correction yields  $\Gamma(\omega) = g^2 \omega^3 / (6\pi v_F^2 v_\Delta^2)$ , where  $v_F$  ( $v_\Delta$ ) is the Fermi (superconducting) velocity at the nodal points perpendicular (parallel) to the Fermi surface. Since for all cases considered below  $\Gamma(\omega_0) \ll \omega_0$ , which requires  $g \ll 50\Delta_0$ ,  $\Gamma(\omega)$  can be neglected and we take for simplicity  $\Gamma(\omega) = 0^+$ . Finally, the LDOS,  $N = A_{11} + A_{22}$  with  $A_{ii}(\mathbf{r}, \omega) = -2\text{Im} \hat{G}_{ii}(\mathbf{r}, \omega + i\delta)$  is obtained numerically from Eqs.(4) with  $\delta = 0.2$  meV.

We showed in Ref. [8] that a single local mode on the surface of a  $d_{x^2-y^2}$ -superconductor is pair-breaking and induces a fermionic resonance state, whose spectroscopic signature are two peaks in the LDOS. Introducing a second mode leads to two new physical effects that introduce *qualitative* changes in the LDOS. First, due to quantum interference of the scattered electrons, the calculation of the LDOS involves not only the local Greens function,  $\hat{G}_0(\mathbf{r}_i, \mathbf{r}_j)$ , and self-energy,  $\hat{\Sigma}(\mathbf{r}_i, \mathbf{r}_j)$ , with  $\mathbf{r}_i = \mathbf{r}_j$ , but also the non-local ones with  $\mathbf{r}_i \neq \mathbf{r}_j$ . As a result, the LDOS is determined by the distance and orientation of the modes relative to the lattice, which is described by  $\Delta\mathbf{r} = \mathbf{r}_i - \mathbf{r}_j = (n_x, n_y)$  (we set the lattice constant  $a_0 = 1$ ). Second, the intermolecular interaction  $\Psi$  leads to characteristic features in the LDOS that, as we show below, depend on the specific form of  $\Psi$ .

In order to distinguish between the effects of quantum interference, superconducting correlations and intermolecular interaction on the LDOS, we consider first a simplified electronic bandstructure with  $t = 300$  meV,

$\mu = t' = 0$  and set  $J = 0$ . In this case, superconducting correlations, as represented by the non-vanishing of the non-local anomalous Greens function,  $F_{\Delta\mathbf{r}}$ , and self-energy,  $\Phi_{\Delta\mathbf{r}}$  (the off-diagonal elements of  $\hat{G}_0$  and  $\hat{\Sigma}_0$ , respectively), are present for  $(n_x + n_y) \bmod 2 = 1$  (*case I*) and vanish otherwise (*case II*). We find that the presence of superconducting correlations leads to qualitative differences in the LDOS between case I and II that are *universal*, i.e., independent of the specific realization of case I or II considered. For definiteness, we consider below two modes located at  $\mathbf{r}_1 = (0, 0)$  and  $\mathbf{r}_2 = (1, 0)$  (case I) and  $\mathbf{r}_1 = (0, 0)$  and  $\mathbf{r}_2 = (2, 0)$  (case II) and present the resulting LDOS at  $T = 0$  in Fig. 1(a) and (b). The

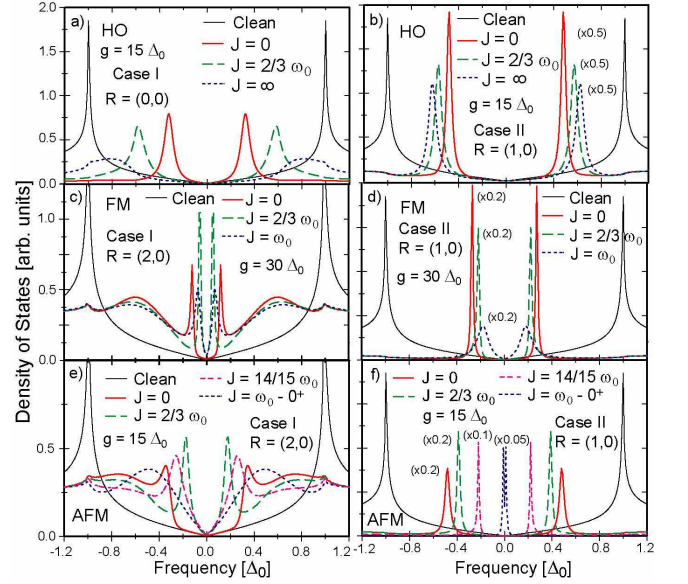


FIG. 1: LDOS at  $\mathbf{R}$  as a function of frequency for  $\omega_0 = 0.6\Delta_0$  and three intermolecular interactions: (a),(b) HO coupling, (c),(d) FM coupling, and (e),(f) AFM coupling. Scaling of the curves is indicated.

coupling of the resonance states due to quantum interference only (see curves for  $J = 0$ ) leads to the formation of bonding and antibonding states and an energy splitting between them. Only one of these states is located at energies smaller than  $\Delta_0$ , resulting in a particle-like and hole-like peak in the LDOS. Quantum interference leads to oscillations in the frequency of the resonance peaks when  $\Delta\mathbf{r}$  is changed (cf. Figs. 1(a) and (b)), similar to the case of non-magnetic impurities [3]. Next, we discuss the effects of three different intermolecular interactions on the frequency and shape of the resonance peaks.

*Harmonic Oscillator (HO) Coupling:* A coupling of the bosonic modes via a quadratic potential is the quantum mechanical analog of two harmonic oscillators coupled by a spring. In this case [9]  $\Psi = (b_{\mathbf{r}_1}^\dagger + b_{\mathbf{r}_1} - b_{\mathbf{r}_2}^\dagger - b_{\mathbf{r}_2})^2$  with  $J \geq 0$ . After diagonalization, one has  $\Omega_1 = \omega_0$ ,  $\Omega_2 = \omega_0 \sqrt{1 + 4\lambda}$  with  $\lambda \equiv J/\omega_0$ ,  $g_{\mathbf{r}_{1,2}}^{(1)} = g/\sqrt{2}$  and  $g_{\mathbf{r}_{1,2}}^{(2)} = \pm g/[\sqrt{2}(1 + 4\lambda)^{1/4}]$ . The re-

sulting LDOS for several values of  $J$  is shown in Fig. 1(a) and (b) for cases I and II, respectively. With increasing  $J$ ,  $\Omega_2$  increases while  $|g_{\mathbf{r}_{1,2}}^{(2)}|$  decreases, the electronic scattering hence becomes weaker and the resonance peaks are shifted to higher energies. In case I, the peaks move close to  $\pm\Delta_0$  as  $J$  increases from  $J = 0$  to  $J = \infty$ , an effect that is independent of  $g$  and directly related to a non-zero  $F_{\Delta r}$  and  $\Phi_{\Delta r}$ . In contrast, in case II, the frequency shift is much smaller. For  $J = \infty$ , only the bosonic *in-phase* mode couples to the fermionic system. This coupling is much weaker in case I than in case II due to the superconducting correlations.

*Ferromagnetic (FM) Coupling:* A second type of intermolecular interaction arises if each molecule possesses  $(2L+1)$  states that are represented by pseudo-spins  $\mathbf{L}_{1,2}$ , whose interaction is given by the anisotropic Heisenberg Hamiltonian

$$H_{spin} = J_z L_1^z L_2^z + J_{\pm} (L_1^x L_2^x + L_1^y L_2^y) . \quad (8)$$

For  $J_z < 0$  and  $|J_z| > |J_{\pm}|$ , the pseudo-spins are ferromagnetically aligned (i.e., the molecules prefer to be in the same state). Performing a Holstein-Primakoff transformation followed by a large- $L$  expansion up to order  $O(L)$ , we obtain  $H_b$  in Eq.(1) with  $\omega_0 = -J_z S > 0$ ,  $J = J_{\pm} S \geq 0$  and  $\Psi = b_{\mathbf{r}_1}^{\dagger} b_{\mathbf{r}_2} + b_{\mathbf{r}_2}^{\dagger} b_{\mathbf{r}_1}$ . After diagonalization, one has  $\Omega_{1,2} = \omega_0 \mp J$ ,  $g_{\mathbf{r}_{1,2}}^{(1)} = \mp g/\sqrt{2}$  and  $g_{\mathbf{r}_{1,2}}^{(2)} = g/\sqrt{2}$ . The operators  $b_{\mathbf{r}_i}^{\dagger}, b_{\mathbf{r}_i}$  represent the excitations of the pseudo-spin dimer which scatter fermions via  $H_{int}$ . For  $J_z < J_{\pm}$ , i.e.,  $J > \omega_0$ , the system becomes unstable since the ferromagnetic alignment of the pseudo-spins is destroyed.

For small values of  $g$ , the resonance peaks move towards lower energies in cases I and II with increasing  $J$  (not shown). However, for intermediate  $g \approx 30\Delta_0$ , this behavior changes qualitatively for case I; the resonance frequencies exhibit a non-monotonic dependence on  $J$  [Fig. 1(c)], in contrast to case II [Fig. 1(d)]. For even larger  $g$ , the resonance peaks shift to higher energies in case I, and to lower energies in case II with increasing  $J$ . A detailed analysis shows that this qualitative difference arises from a non-zero  $F_{\Delta r}$  and  $\Phi_{\Delta r}$  in case I. Note, in case II (Fig. 1(d)), the width of the resonance peaks increases when it shifts to lower energies, in contrast to the effect expected from a decreasing residual DOS [3]. Here, however, the width of the resonance peaks is also determined by the imaginary part of the self-energy which vanishes for  $|\Omega| < \Omega_1$ . Since  $\Omega_1$  decreases with increasing  $J$ , the resonance state becomes more strongly damped once  $\Omega_1 < \omega_{res}$ . In Fig. 1(d), we have  $\Omega_1 = \omega_0 > \omega_{res}$  for  $J = 0$ , but  $\Omega_1 < \omega_{res}$  for  $J = 2\omega_0/3$  ( $\Omega_1 = 0.2\Delta_0$ ) and  $J = \omega_0$  ( $\Omega_1 = 0$ ), resulting in an increased peaks' width for the latter two values of  $J$ .

*Antiferromagnetic (AFM) Coupling:* For antiferromagnetic alignment of the pseudo-spins ( $J_z > 0$ ,  $|J_z| > |J_{\pm}| > 0$  in Eq.(8)), the molecules prefer to be in "op-

posite" states. Performing a Holstein-Primakoff transformation followed by a large- $L$  expansion, one obtains  $\Psi = b_{\mathbf{r}_1}^{\dagger} b_{\mathbf{r}_2}^{\dagger} + b_{\mathbf{r}_1} b_{\mathbf{r}_2}$  resulting in two degenerate energy dispersions  $\Omega_{1,2} = \omega_0 \sqrt{1 - \lambda^2}$  with  $\lambda \equiv J/\omega_0$ ,  $g_{\mathbf{r}_1}^{(1,2)} = \pm g u_{1,2}$ ,  $g_{\mathbf{r}_2}^{(1,2)} = \mp g u_{2,1}$  and  $u_{1,2}^2 = [1/\sqrt{1 - \lambda^2} \pm 1]/2$ . For  $J > \omega_0$ , i.e.,  $|J_z| < J_{\pm}$ , the system becomes unstable since the antiferromagnetic alignment of the molecular pseudo-spins is destroyed.

With increasing  $J$ ,  $\Omega_{1,2}$  decreases while  $g_{\mathbf{r}_2}^{(1,2)}$  increases, thus leading to an increase in the scattering strength. As a result, the resonance peaks shift monotonically to lower energies in case II [see Fig. 1(f)], while their width decreases since  $\omega_{res} < \Omega_{1,2}$  for all  $J$ . In the limit  $J \rightarrow \omega_0$ ,  $g_{\mathbf{r}_2}^{(1,2)}$  diverge, and the scattering becomes unitary. Since the local and non-local  $\hat{G}_0$  and  $\hat{\Sigma}$  vanish for  $\omega = 0$ , the resulting resonance peaks are located at zero energy and the LDOS vanishes at the molecules' sites. In contrast, in case I [Fig. 1(e)], the resonance peaks first shift to lower energies with increasing  $J$ , but eventually move back to higher energies and broaden. This behavior arises from the nonvanishing of the non-local Greens function and self-energy for  $\omega = 0$ .

At  $T = 0$ , the imaginary part of the normal self-energy (the diagonal element of  $\hat{\Sigma}_0$ ) possesses logarithmic divergences that lead to dips in the LDOS at  $\pm\omega_{1,2}^+$  ( $\omega_{1,2}^{\pm} = \Delta_0 \pm \Omega_{1,2}$ ) [8, 10]. At  $T \neq 0$ , the positive energy levels of the bosonic modes, represented by the first term in Eq.(7), become populated, opening a new channel for fermionic scattering. As a result,  $\hat{\Sigma}_0$  acquires logarithmic divergences at  $\pm\omega_{1,2}^-$ . This leads to either peaks or dips in the LDOS, depending on whether  $\omega_i^-$  is smaller or larger than the frequency of the resonance peaks,  $\pm\omega_{res}$ . The LDOS for  $T \neq 0$  is shown in Fig. 2. In Figs. 2(a) and (b), we plot the LDOS for HO coupling

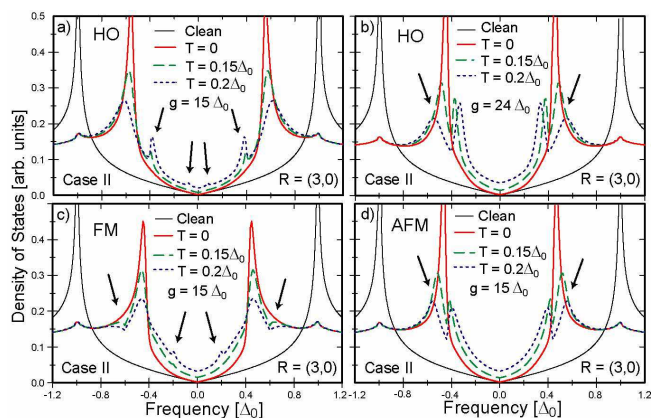


FIG. 2: Temperature dependence of the LDOS for  $\omega_0 = 0.6\Delta_0$  and  $J = 2\omega_0/3$ : (a), (b) HO-coupling, (c) FM-coupling, and (d) AFM-coupling.

in case II for  $g = 15\Delta_0$  and  $g = 24\Delta_0$ , respectively. For  $g = 15\Delta_0$ ,  $\omega_{1,2}^- < \omega_{res}$  and the logarithmic divergences

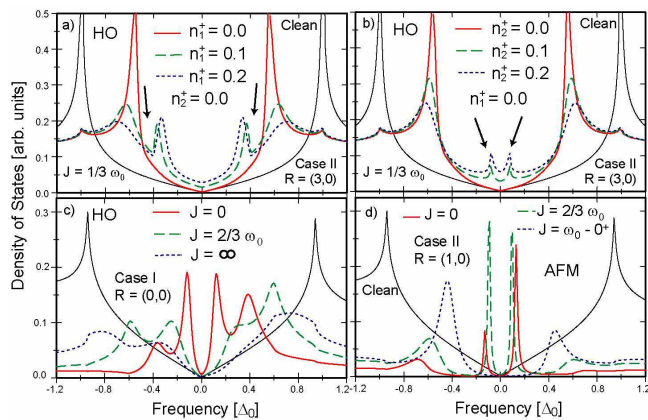


FIG. 3: LDOS at  $T = 0$  for  $\omega_0 = 0.6\Delta_0$  and  $g = 15\Delta_0$ . (a),(b) The positive energy branches of the bosonic modes are selectively populated for HO-coupling with  $n_{1,2}^- = 1$  and  $J = \omega_0/3$ . (c), (d) LDOS for a HTSC band structure and (c) HO-coupling, and (d) AFM-coupling.

lead to four peaks (indicated by arrows) in the LDOS. Their intensity is governed by  $n_B(\Omega_i)$  and thus larger at  $\pm\omega_1^-$  than at  $\pm\omega_2^-$ . Simultaneously, opening of the new scattering channels leads to an increase in the imaginary part of the self-energy, resulting in a shift of the resonance peaks to higher energies and an increase in their width. In contrast, for  $g = 24\Delta_0$ ,  $\omega_1^- \approx \omega_{res}$ , leading to a splitting of the resonance peaks and to a dip in the LDOS. The second set of divergences at  $\omega_2^-$  induces two peaks in the LDOS, which due to the overall increase in the LDOS at lower energies are barely perceptible. The LDOS for FM coupling and AFM coupling in case II is shown in Fig. 2(c) and (d), respectively. For FM coupling, the LDOS exhibits two peaks and two dips since  $\omega_1^- < \omega_{res} < \omega_2^-$ . In contrast, for AFM coupling, the two modes are degenerate and since  $\omega_{1,2}^- > \omega_{res}$ , the logarithmic divergences result in a single set of dips. The LDOS in case I (not shown) exhibits qualitatively similar behavior to the ones discussed above for all three couplings. Note that the frequencies of the features arising from the logarithmic divergences are *independent* of  $g$ , which thus permits a direct measurement of  $\pm\omega_{1,2}^\pm$ .

The degeneracy of the modes for AFM coupling results in a LDOS with only two features at  $\pm\omega_1^-$  and  $\pm\omega_1^+$ , respectively, in *qualitative* contrast to the LDOS for FM and HO coupling. The latter two couplings, however, can be distinguished by comparing  $\omega_0$  obtained from the LDOS near a single molecule [8] with  $\omega_{1,2}^\pm$ . Thus the nature of the intermolecular interaction, similar to a molecule's internal structure [6], can be identified experimentally from the specific features it induces in the LDOS.

Changing the population,  $n_{1,2}^\pm$ , of the energy levels  $\pm\Omega_{1,2}$ , for example by optical means [11], opens intriguing venues to manipulate the local electronic structure of the host material. In Fig. 3(a),(b), we present the LDOS

for HO coupling with  $n_{1,2}^- = 1$  and  $n_{1,2}^+ \neq 0$ . A non-zero  $n_1^+$  [Fig. 3(a)] induces dips in the LDOS at  $\pm\omega_1^-$ , while an increase of  $n_2^+$  [Fig. 3(b)] leads to peaks at  $\pm\omega_2^-$ , similar to the temperature induced changes discussed above.

Finally, the use of a bandstructure representative of the HTSC with  $t'/t = -0.4$  and  $\mu/t = -1.18$  [12] mixes the effects of intermolecular interaction, superconducting correlations and quantum interference on the LDOS. For example, the  $J$ -dependence of the LDOS for HO coupling [Fig. 3(c)] is similar to the one shown in Fig. 1(a), while the LDOS for AFM coupling [Fig. 3(d)] shows a dependence on  $J$  that is qualitatively different from that in Fig. 1(f).

In conclusion, we study the effects of molecular nanostructures on the electronic structure of a  $d_{x^2-y^2}$ -wave superconductor. We show that different intermolecular interactions lead to *qualitatively* distinguishable signatures in the LDOS. By changing the population of the bosonic excitations, one can manipulate the host's electronic structure and gain further insight into the nature of unconventional superconducting correlations.

We would like to thank J.C. Davis, T. Imbo, and K.-H. Rieder for stimulating discussions. D.K.M. acknowledges support from the Alexander von Humboldt foundation.

- 
- [1] H.C. Manoharan *et al.*, Nature (London) **403**, 512 (2000); K.-F. Braun and K.-H. Rieder, Phys. Rev. Lett. **88**, 096801 (2002); D.J. Hornbaker *et al.*, Science **295**, 828 (2002); G.V. Nazin *et al.*, Science **302**, 77 (2003).
  - [2] D.K. Morr and N.A. Stavropoulos, Phys. Rev. B **67**, 020502(R) (2003); *ibid.* Phys. Rev. Lett **92**, 107006 (2004).
  - [3] D.K. Morr and N.A. Stavropoulos, Phys. Rev. B **66**, 140508(R) (2002); L.Y. Zhu *et al.*, Phys. Rev. B **67**, 094508 (2003); B.M. Andersen and P. Hedegard, Phys. Rev. B **67**, 172505 (2003).
  - [4] R.C. Jaklevich and J. Lambe, Phys. Rev. Lett. **17**, 1139 (1966); B.C. Stipe, M.A. Rezaei, and W. Ho, Science **280**, 1732 (1998); J.K. Gimzewski and C. Joachim, Science **283**, 1683 (1999).
  - [5] For recent reviews see D. Drakova, Rep. Prog. Phys. **64**, 205 (2001); A. Nitzan, Annu. Rev. Phys. Chem., **52**, 681 (2001); W. Ho, J. Chem. Phys. **24**, 11033 (2002), and references therein.
  - [6] L. Gross *et al.*, Phys. Rev. Lett **93**, 056103 (2004)
  - [7] A.C. Hewson and D.M. Newns, J. Phys. C: Solid State Phys. **12**, 1665 (1979).
  - [8] D.K. Morr and R.H. Nyberg, Phys. Rev. B **68**, 060505(R) (2003)
  - [9] C. Cohen-Tannoudji *et al.*, *Quantum Mechanics Vol. I* (Wiley, 1977), Chap. 5.
  - [10] A.V. Balatsky, Ar. Abanov, and J.-X. Zhu, Phys. Rev. B **68**, 214506 (2003).
  - [11] S. Nie and S.R. Emory, Science **275**, 1102 (1997); K. Kneipp *et al.*, Phys. Rev. Lett. **78**, 1667 (1997).
  - [12] A. Damascelli, Z. Hussain, and Z.-X. Shen, Rev. Mod. Phys. **75**, 473 (2003).